Prediction of Depth Ratio, Jump Length and Energy Loss in Sloped Channel Hydraulic Jump for Environmental Sustainability

Sanjeev Kumar Gupta
Department of Mechanical Engineering, IET, GLA University Mathura

Vijay Kumar Dwivedi
Department of Mechanical Engineering, IET, GLA University Mathura

https://doi.org/10.5109/6792889

出版情報：Evergreen. 10 (2), pp.942-952, 2023-06. 九州大学グリーンテクノロジー研究教育センター
バージョン：

Prediction of Depth Ratio, Jump Length and Energy Loss in Sloped Channel Hydraulic Jump for Environmental Sustainability

Sanjeev Kumar Gupta[1,*], Vijay Kumar Dwivedi[1]

[1]Department of Mechanical Engineering, IET, GLA University Mathura, India-281406

E-mail: sanjeev.mnnita@gmail.com

(Received February 19, 2023; Revised March 28, 2023; accepted April 17, 2023).

Abstract: The association of enormous amounts of energy proximate to hydraulic structures, like spillways, downstream of draft tubes, etc., which might be harmful to environment, has prompted the researcher to consider this occurrence to dissipate this excess energy. Due to natural occurrence, hydraulic jump unavoidably reduces incoming flow energy. Most of the researchers considered hydraulic jump characteristics to be the function of inflow Froude number but in this research, the effects of incoming Reynolds number (Re1) is introduced first time in a sloped channel jump and all the correlation are formed while taking into account the influence of Re1, inflow Froude number (Fr1) and Channel slope (θ). The experiment was performed in the sloped channel (0^0, 2^0, 4^0 and 6^0) in an open channel flow test setup and eight experiments are designed and performed and collected 57 data for each channel slope. Regression analysis was utilised after using Buckingham's theorem to make all the variables dimensionless to generate correlations. Moreover, error analysis was carried out, and all created correlations were compared to correlations that had already been developed. The depth ratio (d_2/d_1) increases by 34.85%, relative length (L_j/d_1) decreases by 18.91% and energy loss (E_L/E_1) increases by 63.62% for 6^0 channel slope as compared to the classical jump. The R^2 value of developed correlation for d_2/d_1, L_j/d_1, L_j/d_1 (in terms of d_1/d_2) and E_L/E_1 was 0.98, 0.975, 0.98 and 0.99 respectively which shows the efficacy of the entire developed model.

Keywords: Energy dissipation; Sloped channel; Froude number; Reynolds number; Hydraulic jump, Environmental sustainability

1. Introduction

Research on hydraulic jumps has been ongoing for millennia since they are such an amazing phenomenon[1)2)3)]. One of the top priorities for hydraulic engineers is energy dissipation after hydraulic construction. The goal of creating energy dissipaters is to diminish some of the kinetic energy of the inflowing stream, which could cause corrosion and undermine the support of the hydraulic structural system, inevitably resulting in their destruction[4)5)6)]. The attraction with hydraulic jumps is related to their ferocity and the intricate relationships between roller formation, instabilities, and instability that makes them effective energy dissipaters[7)8)]. The various effects and applications of the hydraulic jump are illustrated in figure 1.

A flow regime change from torrential (supercritical) to subcritical to calm stream with massive energy loss and an increase in flow depth causes the phenomena called a hydraulic jump. A flow is said to be supercritical when Froude number (Fr) is greater than one. The primary function of hydraulic jump is to disperse surplus energy from moving water[9)10)]. The kinetic energy of a rapidly moving stream is transformed into potential energy by hydraulic jumps. There is a loss of kinetic energy as a result. Rollers of turbulent water arise where hydraulic jumps happen, dissipating energy[11)12)13)].

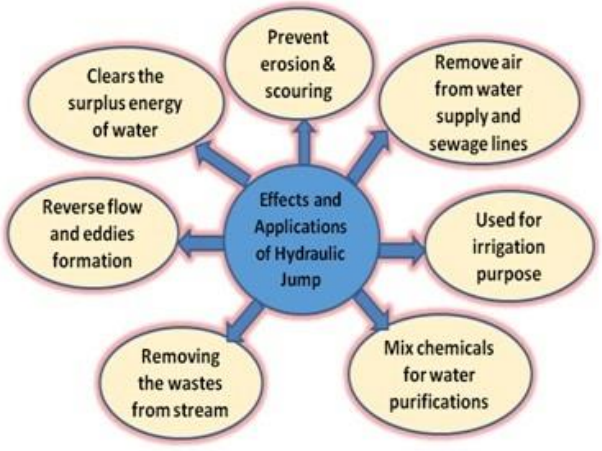

Fig. 1: Effects and applications of hydraulic jump

If this surplus energy is not contained, the banks and the bed will suffer. Environmental protection and its sustainability are a major concern now these days. When the hydraulic jump happens, a sizable quantity of air is often entrapped in the water. By using that air, it may be possible to remove the wastes from the streams that are harming the ecosystem. Air can be removed from water supply and sewage lines using the hydraulic jump to prevent air locking[14)15)].

A hydraulic jump needs a supercritical flow to happen. An essential dimensionless parameter in the investigation of hydraulic jump is the Froude number. As the Froude number rises, the jump becomes more chaotic and loses more energy. Only when the Froude number is greater than one can a jump take place[16)17)18)]. The square root of the inertia force to the gravitational force is known as the Froude number (Fr). Mathematically it is expressed as[19)]

$$F_r = V/\sqrt{gd} \tag{1}$$

Leonardo Da Vinci originally drew and wrote about the hydraulic jump phenomenon over 500 years ago. It is thought that Belanger's (1849) development of the subsequent depth ratio for a free hydraulic jump in a horizontal channel was the first study on the hydraulic jump[19)].

$$\frac{Y_2}{Y_1} = \frac{1}{2}\left(\sqrt{1+8F_{r_1}^{\ 2}} - 1\right) \tag{2}$$

By conducting observations in a channel that was slightly expanding, Ellms tested the first theoretical theory on the hydraulic jump in a sloping channel. Ellms constructed an equation for subsequent depth ratio as Newton's second rule of motion, disregarding the weight effect[20)].

$$\frac{d_2}{d_1} = \pm\left[\frac{2}{3}F_{r_1}^{\ 2}\cos\theta + \frac{1}{3\cos\theta}\right]^{1/2} \tag{3}$$

Concerning the initial Froude number, Bradley and Peterka[21)] constructed a correlation for the jump's length and relative energy loss in a rectangular channel as

$$\frac{L_J}{Y_2} = 220\tanh\left(\frac{F_{r_1}-1}{22}\right) \tag{4}$$

$$\frac{E_L}{E_1} = 1 - \frac{\frac{Y_2}{Y_1} + \frac{F_{r_1}^{\ 2}}{2\left(\frac{Y_2}{Y_1}\right)^2}}{1+\frac{F_{r_1}^{\ 2}}{2}} \tag{5}$$

Using the momentum equation, Chow[22)] developed the following analytical expression for the subsequent depth ratio in a sloping channel:

$$\frac{d_2}{d_1} = \frac{1}{2}\left(\sqrt{1+8G^2} - 1\right) \tag{6}$$

Where

$$G = \frac{F_{r_1}}{\sqrt{\cos\theta - \frac{KL_j\sin\theta}{d_2 - d_1}}}, \quad F_{r_1} = \frac{V_1}{\sqrt{gd_1\cos\theta}} \text{ and}$$

K is the shape factor.

On corrugated beds, hydraulic jumps were studied by Ead and Rajaratnam[23)]. They discovered that the needed tail water depth for the formation of a jump was significantly lower compared to the same jump on a flat channel. In addition, the jumps' length was also nearly half that of jumps on the flat channel. Hydraulic jumps on steep slopes were studied conceptually as well as experimentally by Pagliara et al.[24)]. Based on the findings, it was determined that a sill stabilized the hydraulic jump. Beirami et al.[25)] have looked into the characteristics of hydraulic jumps over sloping beds. They experimented on four different channel slopes. They concluded that the classical jump lost more energy than any other jump that formed on either a positive or negative slope. Their experimental study revealed that the depth ratio (d_2/d_1) was reduced by the basin's negative slope. However, a positive channel slope raises the depth ratio. Pagliara et al.[26)] performed experimentation on a negatively sloped bed, taking into account the impact of air entrainment. They concluded that a fall in depth ratio results from a rise in shear stresses brought on by bed roughness. In addition, it was suggested to use a theoretical model to calculate the depth ratio in a variety of structural and boundary arrangements. Palmero et al.[27)] experimented on D-jump in a sloped channel. They have developed a correlation for the sequent depth of the D-jump. Additionally, it was demonstrated experimentally that the effect of channel bed roughness on the subsequent depth ratio depends mostly on the relative roughness at relatively low channel slopes. Abbaspour et al.[28)] performed experimentation on the hydraulic jump with a reverse bed using porous screens. The Froude number during experimentation varied from 4.5 to 10.6. The screens were examined with roughly 50% porosity and square holes. According to the study's findings, utilising screens on an inverse slope of 0.025 expends more energy than doing so on an inverse slope of 0.015. Luo et al.[29)] presented a technique on a sloped channel to detect the jump sole. A crucial element for a slab stability study of a sluice stilling basin with a sloping connecting section is provided by the method. A way to determine a sluice's SCS stability was presented based on this approach. The approach has the drawback of not taking the jump's dynamic effect into account. If this effect predominates, the procedure might not be appropriate. Parsamehr et al.[30)] experimented on an adverse slope for

hydraulic jumps controlled by roughness elements. The Froude number during experimentation varied from 4.9 to 12.4. According to the findings, a smooth bed would have a bed shear coefficient that was 12.4 times greater on average on a negative slope. When roughness components and negatively sloped height rose, the decline became more noticeable. They also obtained the value of G from equation 6 from their experimental observation as

$$G = 0.996e^{-3.878\tan\theta}F_{r_1},\ R^2=0.999 \quad (7)$$

Despite the extensive study being done on the traditional hydraulic jump in the horizontal channel, the hydraulic jump in a sloping channel has not received the required attention. A hydraulic jump in the sloped channel increases the energy dissipation which is ultimately required to reduce the adverse effect of this phenomenon for environmental sustainability. Most of the researchers considered hydraulic jump characteristics to be the function of inflow Froude number but the first-time effect of inflow Reynolds number on jump characteristics was also introduced in the present investigation. The goal of the current study is to increase understanding of hydraulic jumps on sloping channels and make further attempts to produce new empirical correlations taking into account the influence of both inflow Froude number and inflow Reynolds number that might be useful in evaluating the different jump characteristics that can be useful in designing stilling basins and minimising the negative effects of hydraulic jump on the environment.

2. Analysis of Sloped Channel Hydraulic Jump

2.1 Theoretical Analysis

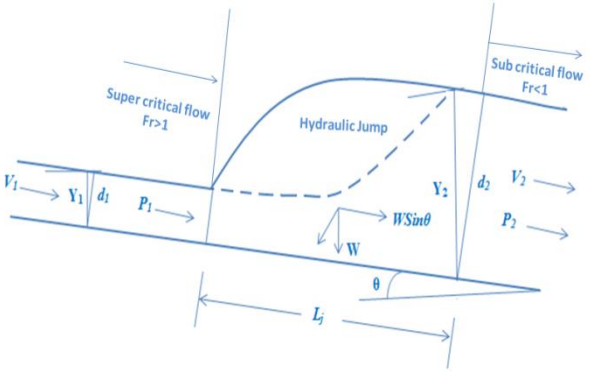

Fig. 2: Analysis of sloped channel hydraulic jump

The channel bed in this kind of hydraulic jump is positioned at an angle to the horizontal axis. The general momentum equation can be used to describe a hydraulic jump in a channel with a sloped floor. Without further information, it is impossible to solve the momentum equation because there are too many unknown terms concerning the number of equations that are accessible. The term Wsinθ, which denotes the longitudinal component of water's weight in the jump, presents a challenge because it is an unknown quantity. This is because Wsinθ incorporates the jump's length and profile, details of which can only be learned through experimental observation. A rectangular channel with a unit width is assumed for the investigation of the jump in a sloping channel and is depicted in fig. 2. The channel bottom is assumed to be parallel to all effective forces.

The momentum equation is expressed as follows when applying hydrostatic pressure force in the direction of flow in sloping channels and considering a rectangular channel of unit width:

$$P_1 - P_2 + WSin\theta = \rho q(V_2 - V_1) \quad (8)$$

Where $P_1 = \frac{1}{2}\rho g d_1^{\,2}\cos\theta$, $P_2 = \frac{1}{2}\rho g d_2^{\,2}\cos\theta$

$Y_1 = d_1\cos\theta$ and $Y_2 = d_2\cos\theta$

The weight of the water in the jump can be described as follows if the surface profile of the jump is considered to be a straight line[31]:

$$W = \frac{1}{2}\rho g L_j (d_1 + d_2) \quad (9)$$

The energy per unit weight of the water measured concerning the channel bed is known as specific energy. In consideration of the water's weight, specific energy is calculated as

$$E_1 = d_1\cos\theta + \frac{V_1^2}{2g} + L_j\sin\theta \quad (10)$$

$$E_2 = d_2\cos\theta + \frac{V_2^{\,2}}{2g} \quad (11)$$

2.2 Dimensional Analysis

According to jump characteristics in sloped channels, the key variables influencing the jump phenomenon are expressed as a function of

$$f\begin{pmatrix} d_1, d_2, H_j, V_1, V_2, L_j, E_1, E_2 \\ , E_L, \rho, g, \mu, \varepsilon, \eta, \theta \end{pmatrix} \quad (12)$$

Since there are fifteen variables (dependent and independent) and these variables contains three fundamental dimensions (M, L and T), therefore these variables are organized into twelve dimensionless terms in accordance with Buckingham's π theorem which is provided in equation 13.

The following dimensionless groups are created by π-theorem and treating d_1, V_1, and ρ as repeating variables.

$$f_1\left(\frac{d_2}{d_1},\frac{L_j}{d_1},\frac{H_j}{d_1}\frac{E_L}{d_1\cos\theta},\frac{E_1}{d_1\cos\theta},\frac{E_2}{d_1\cos\theta},\frac{E_2}{E_1},\frac{E_L}{E_1},\frac{V_2}{V_1},\frac{V_1^{\,2}}{gd_1\cos\theta},\frac{\rho V_1 d_1\cos\theta}{\mu},\frac{\varepsilon}{d_1\cos\theta}\right)=0 \quad (13)$$

The approach Froude number (Fr_1), the approaching Reynolds number (Re_1) and the channel slope are revealed to be the primary determinants of depth ratio, relative jump length, and relative energy loss which may be written as:

$$\frac{d_2}{d_1}=f_3\left(F_{r1},R_{e1},\theta\right) \quad (14)$$

$$\frac{L_j}{d_1}=f_4\left(F_{r1},R_{e1},\theta\right) \quad (15)$$

$$\frac{E_L}{E_1}=f_5\left(F_{r1},R_{e1},\theta\right) \quad (16)$$

3. Instrumentation and Experimental Methodology

The experiments were conducted in the Fluid Mechanics Laboratory of the Civil Engineering Department of GLA University Mathura utilising a transparent Perspex sheet flume. Figure 3 depicts the general design of the experimental setup.

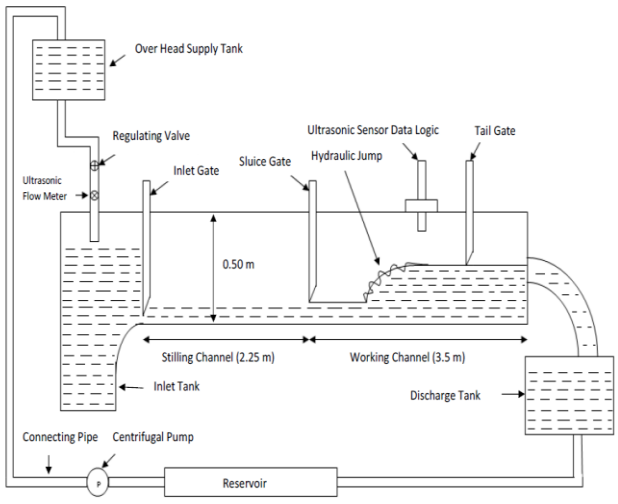

Fig. 3: Schematic view of the experimental set-up

To reduce mistakes caused by changes in flow during testing, a constant head supply tank with a volume of 3.7 x 3.7 x 3.2 m^3 is offered. A centrifugal pump delivers water through a connecting pipe with a diameter of 15 cm that is equipped with a regulating valve to the inlet tank, which has a volume of 0.50 x 0.50 x 0.85 m^3. At the upper end of the working section, a stilling channel with dimensions of 2.25 m length 0.45 m width, and 0.50 m height is provided to ensure even flow distribution. The experiments were performed in a 3.5 m long channel that was 0.45 m wide and 0.50 m tall.

For even flow and to reduce the creation of turbulence and eddies, the bottom surface is built of cement. Perspex side walls are used to visualise the starting and landing positions of jumps. The top of the side walls is mounted with parallel rails that allow the Data Logic US30 ultrasonic sensor having ± 0.1 mm accuracy and 10-100 cm operating range to slide along them as it measures the depth at various points throughout the length and width of the channel. To control the depth of flow entering the working part, a movable, vertical regulating gate with sharp edges is employed at the upper and lower portion of the working channel. To gather the water released from downstream of the channel, a collecting tank is provided. With an accuracy range of 0.7% to 1%, the discharge in the flume was monitored by an ultrasonic flow meter. The channel is positioned at various angles to facilitate experimentation in the sloped channel.

In both a horizontal and sloping rectangular channel, free hydraulic jump experiments were conducted. By opening and closing the tailgate and sluice gate repeatedly at different discharge levels, a jump was produced. Initial depth, sequent depth, and hydraulic jump length were all measured for each run. The aforementioned actions were carried out in the order listed above at various valve openings for various channel slopes. Fig. 4 represents the formation of a hydraulic jump in a sloped channel.

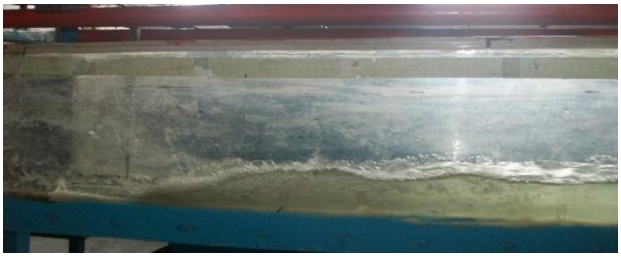

Fig. 4: Formation of hydraulic jump in sloped channel

By adjusting the downstream tail water depth and inflow conditions, 55 experiments were carried out for each channel slope. Table 1 (appendix) displays an overview of the experiment's findings. The Froude number (Fr) during experimentation varied from 2.5 to 8.5 and the Reynolds number (Re) varied from 5100 to 26000. The slope of the bed varied from 2^0 to 6^0.

The error associated with all measuring instruments and all the jump characteristics is provided in table 2.

Table 2 Error associated with instruments and jump characteristics

S. No.	Instruments/Hydraulic Jump characteristics	% Error
1	Data Logic US30 ultrasonic sensor	0.1%
2	Ultrasonic flow meter	0.7% to 1%
3	Sequent Depth Ratio (d_2/d_1)	±10%
4	Length of Jump (L_j/d_1)	±15%
5	Energy Loss due to Jump (E_L/E_1)	±10%

4. Result and Discussion

4.1 Sequent Depth Ratio

The plot of depth ratio with Froude number for different bed slopes is shown in the figure. 5. It shows that with the rise in Froude number, sequent depth ratio (d_2/d_1) rises linearly for all experiments from 0^0 to 6^0 and also shows that for 0^0, 2^0, 4^0, and 6^0 channel bed slopes, respectively, 96%, 99%, 97%, and 99% of data points are well inside ±10% of the trend line with a determination coefficient (R^2) values of 0.96, 0.98, 0.98, and 0.974. Some experimental data depart from the trend line, which could be the result of inaccurate flow depth measurements. It is also evident from fig. 5, equation 3 and equation 6 that the depth ratio increases linearly with the rise in Froude number and bed slope. Utilizing regression analysis of experimental data and Buckingham's π theorem, the following empirical correlation was created taking into account the effects of Fr_1, Re_1, and channel slope θ.

$$\frac{d_2}{d_1} = 812\left(\frac{F_{r1}^{2.5}}{R_{e1}}\right) + 24\tan\theta + 3.456,\ R^2=0.98 \quad (17)$$

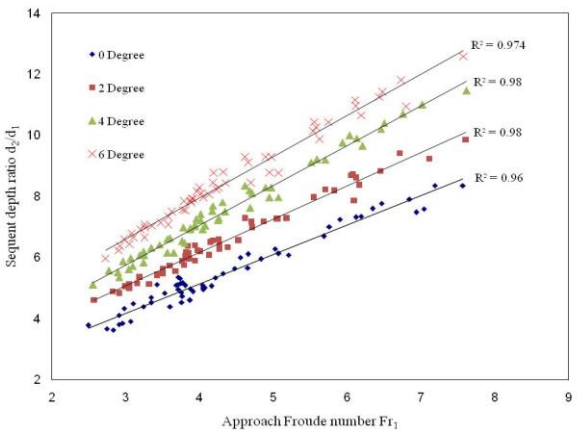

Fig. 5: Variation of d_2/d_1 with Fr_1 for all channel slopes

It is found from correlation 17 that depth ratio (d_2/d_1) increases with Fr_1 and channel slope θ while decreases with Re_1.

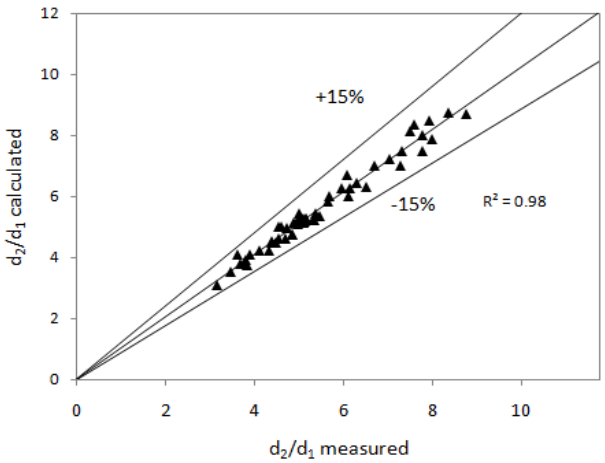

Fig. 6: Plot of calculated value of d_2/d_1 from regression-based model equation 17 and measured value d_2/d_1 from experimental data

The calculated value of d_2/d_1 from regression-based model equation 17 and measured value d_2/d_1 from experimental data coincide quite well, as shown in Figure 6. Every data values are well inside ±15% of the trend line, and the linear fit of measured and calculated values of d_2/d_1 with R^2 = 0.982 shows that the current model equation 17 fits the data well. The present developed model of sequent depth ratio (d_2/d_1) is compared with the previously developed model by Pagliara 2015[26], Pourabdollah 2019[3] and Parsamehr 2022[30] which is shown in figure 7. The value of regression coefficient R^2 of the present model equation is 0.989 which is good as compared to other developed models which show the efficacy of the present model equation. The depth ratio can be estimated quite accurately given the intricacy of the jump phenomenon.

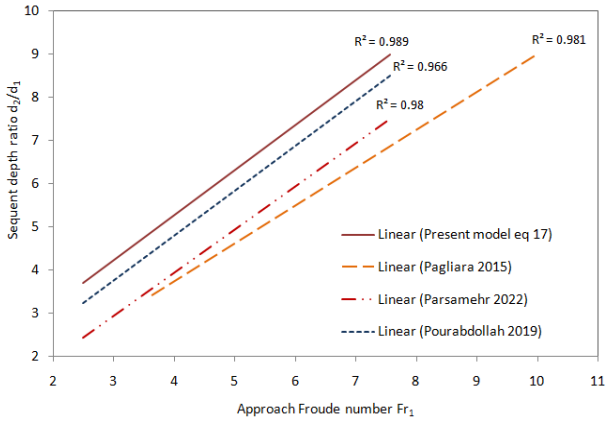

Figure 7 Comparison of the presently developed model of sequent depth ratio with other developed model

4.2 Length of the Jump

Another crucial element of the hydraulic jump is the length of the surface roller. The distance between the jump's toe and the roller end is known as the roller length (Lr). The roller length is a more appropriate characteristic to assess because determining the jump

length might be challenging due to surface waves. The assumption is that the roller length corresponds to the jump length for adversely inclined beds, both smooth and rough[32)33)]. Carollo et al.[34)] developed a correlation for relative roller length (Lr/d_1) considering the effect of depth ratio. This equation is further validated using the experimental data of Hager et al.[35)].

$$\frac{L_r}{d_1} = 4.078\left(\frac{d_2}{d_1} - 1\right) \tag{18}$$

Eq. (18) provides a good estimate of the dimensionless roller length, taking into account the complexity of the phenomena. Hager[20)] also developed an empirical correlation for Lr/d_1 as a function of Fr_1 for a sloped channel which is estimated in equation 19.

$$\frac{L_r}{d_1} = -12 + 100\tanh\left(\frac{F_{r1}}{12.5}\right) \tag{19}$$

Hassanpour et al. [36] performed experimentation on gradually expanding channels and developed a correlation for hydraulic jump characteristics. The most important fact of their study is that they have developed a correlation between the relative roller length as well as the relative length of the jump. The inflow Fr_1 in their study was in the range of 6 to 12. Their model for the relative length of the jump is demonstrated by equation 20. The regression coefficient (R^2) value for their developed model was 0.89.

$$\frac{L_j}{d_1} = 8.924F_{r_1} + 11.473B - 12.39\left(\frac{r}{d_1}\right) - 21.541 \tag{20}$$

Where B is the expansion ratio and r/d_1 is the relative roughness height.

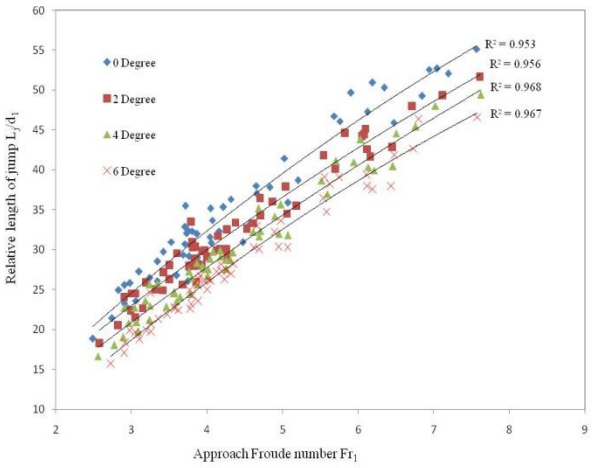

Fig. 8: Variation of L_j/d_1 with Fr_1 for all channel slopes

The plot of relative jump length (L_j/d_1) with Fr_1 is shown in figure 8. It is clear from the experimental observation that L_j/d_1 increases with Fr_1 while decreasing with the slope of the channel θ. Figure 8 indicates that for 0^0, 2^0, 4^0, and 6^0 channel bed slopes, respectively, 94%, 97%, 96%, and 97% points are well inside ±10% of the trend line with a determination coefficient (R^2) values of 0.95, 0.96, 0.97, and 0.97. Based on dimensional analysis L_j/d_1 is found to be a function of the incoming Froude number (Fr_1), Reynolds number (Re_1) and channel slope θ. The regression-based model for L_j/d_1 is given by equation 21 with an R^2 value of 0.975.

$$\frac{L_j}{d_1} = 4678\left(\frac{F_{r1}^{2.2}}{R_{e1}}\right) - 59\tan\theta + 26.064 \tag{21}$$

From correlation 21 of length of jump, it is observed that jump length (L_j/d_1) increases with Fr_1 while decreases with Re_1 and channel slope θ. The values of the relative length obtained from the correlation developed and the experimental measurements coincide quite well, as illustrated in Figure 9. Every data points are well inside the ±15% trend line, and the linear fit of measured and calculated values of L_j/d_1 with $R^2 = 0.975$ shows that the current model equation 21 fits the data well.

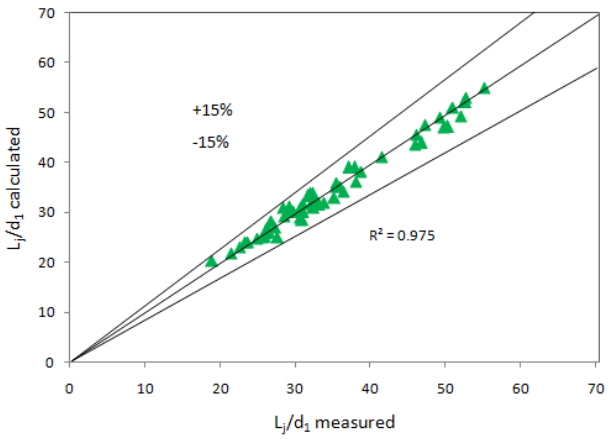

Fig. 9: Plot of the calculated value of L_j/d_1 from regression-based model equation 21 and measured value L_j/d_1 from experimental data

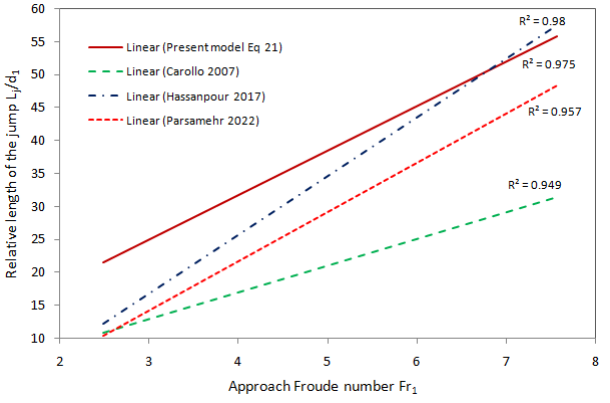

Fig. 10: Comparison of the presently developed model of relative jump length with other developed model

The L_j/d_1 also shows a reasonably good variation with depth ratio (d_1/d_2). In this paper, an attempt is also made to plot this variation which is shown in figure 11 and also developed an empirical correlation provided by equation 22 without considering the effect of inflow Reynolds number. There is a power variation of L_j/d_1 with d_1/d_2 and its decreases with the increase of d_1/d_2 and also decreases with the increase of channel slope. Almost 97% of data are well inside ± 10% of the trend line for all slope channels with an R^2 value of 0.963, 0.969, 0.975 and 0.96 for 0 to 6^0 channel slopes respectively.

$$\frac{L_j}{d_1} = 3.237\left(\frac{d_1}{d_2}\right)^{-1.15} - 46\tan\theta,\ R^2=0.986 \qquad (22)$$

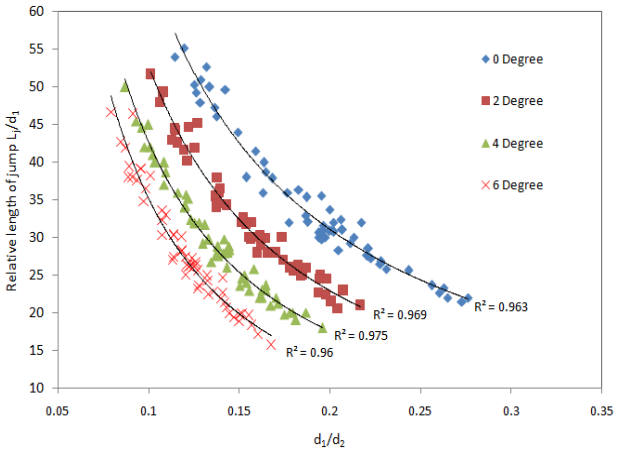

Fig. 11: Variation of L_j/d_1 with depth ratio d_1/d_2

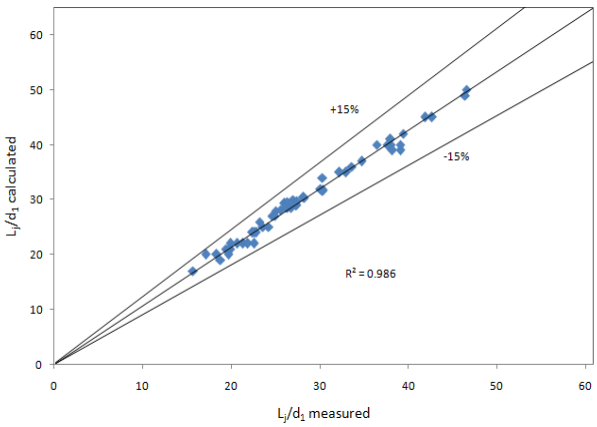

Fig. 12: Plot of the calculated value of L_j/d_1 from the regression-based model equation 22 and measured value L_j/d_1 from experimental data

From correlation 22 of jump length, it is observed that L_j/d_1 decreases with d_1/d_2 as well as channel slope θ. The plot of L_j/d_1 calculated from model equation 22 and L_j/d_1 measured from experimental data is shown in figure 12. Every data points are well inside ±15% of the trend line, and the linear fit of measured and calculated values of L_j/d_1 with R^2 = 0.986 shows that the current model equation 22 fits the data well.

4.3 Energy Loss due to Jump

The loss of energy is a very important parameter in the study of the jump phenomenon because the kinetic energy of the stream is converted into potential energy due to the rise in depth of flow. This energy is converted into turbulent energy and finally into heat energy which is dispersed to the atmosphere[37)38)]. Loss of energy due to jump is the difference of specific energy before the jump and after the jump which is calculated by equations 10 and 11 in the case of the sloped channel. The correlation for relative energy loss (E_L/E_1) developed by Parsamehr et al.[30)] and Hassanpour et al.[36)] is given by Equations 23 and 24.

$$\frac{E_L}{E_1} = -0.003F_{r_1}^{\ 2} + 0.07F_{r_1} + 0.017\frac{r}{d_1} - 0.021S + 0.334 \qquad (23)$$

$$\frac{E_L}{E_1} = 0.250\ln\left(F_{r_1}\right) - 0.024B^2 - 0.023B + 0.026\left(\frac{r}{d_1}\right) + 0.244 \qquad (24)$$

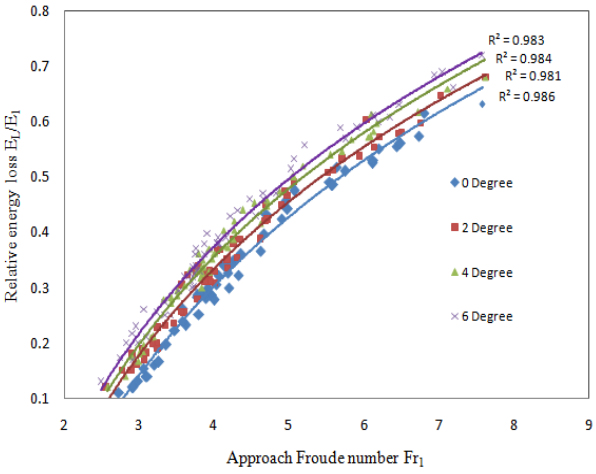

Fig. 13: Variation of E_L/E_1 with depth ratio Fr_1

The plot of the variation of energy loss with Fr_1 is provided in figure 13. The relative energy loss increases logarithmically with Fr_1 as well as with channel slope θ. It is only possible because, at a higher Froude number, the kinetic energy of the stream is high. It is obvious from plot 13 that 98% of experimental data are well inside ±10% of the trend line for all channel slopes. It is found from the experimental observation that energy loss is approximately 15.38%, 35.07% and 63.62% for 2^0, 4^0, and 6^0 channel slopes respectively as compared to

classical hydraulic jump (0^0 bed slopes). From this, we may infer that energy loss increases with increasing bed slope, which is a prerequisite in the case of the hydraulic jump phenomenon to reduce the phenomenon's negative effects on the environment while simultaneously increasing the sustainability of the environment. The experimental-based model equation for the present study considering the effect of Fr_1, Re_1 and θ was defined as equation 25. The variation of the present model equation is logarithmic with an R^2 value of 0.997.

$$\frac{E_L}{E_1} = 0.224 \ln\left(\frac{F_{r_1}^{\,2.5}}{R_{e_1}^{\,0.01}}\right) + 6\tan\theta - 0.452 \qquad (25)$$

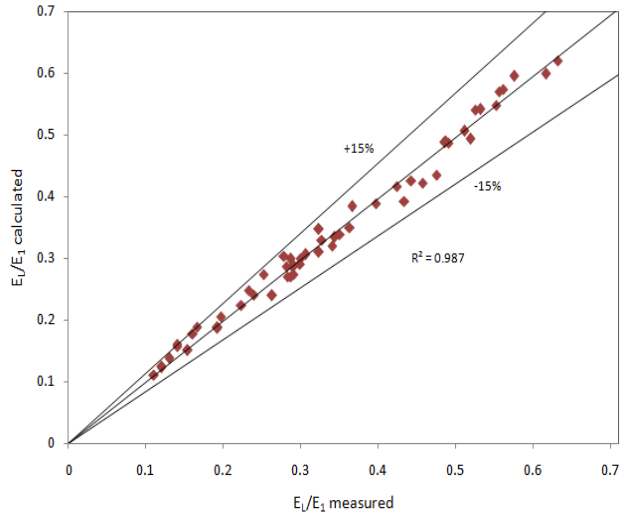

Figure 14 Plot of the calculated value of E_L/E_1 from regression-based model equation 25 and measured value E_L/E_1 from experimental data

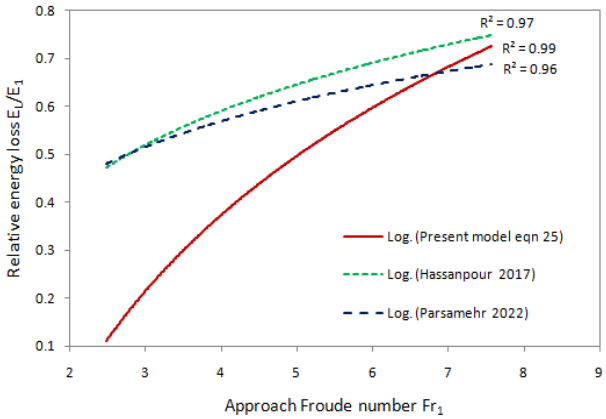

Fig. 15: Comparison of the presently developed model of E_L/E_1 with other developed model

It is clear from correlation 25 of energy loss due to jump (E_L/E_1) rises with rise in Fr_1 and channel slope θ while decrease with Re_1. The plot of E_L/E_1 calculated from model equation 25 and E_L/E_1 measured from experimental data is illustrated in figure 14. Every data points are well inside ±15% of the trend line, and the linear fit of measured and calculated values of E_L/E_1 with $R^2 = 0.987$ shows that the current model equation 25 fits the data well.

The comparison plot of present regression equation 28 with other developed equations of Hassanpour 2017[36] and Parsamehr 2022[30] is shown in fig. 15. The R^2 value of the present equation is 0.99 which is better than other developed models. It shows the usefulness of the present correlation. It is also noticed from figure 15 that very little change in E_L/E_1 with the variation of Fr_1 in the previously developed model but the present model shows reasonably good logarithmic variation with the change of Fr_1 which shows the wide visibility and acceptance of the present model equation.

With increase of channel slope, the sequent depth increases which results in conversion of kinetic energy into potential energy and this potential energy is finally converted into heat energy and dissipated to atmosphere due to this there is a loss of energy. With increase of Froude number, the flow becomes supercritical which results in formation of eddies and flow separation can take place which ultimately results in increment in energy loss.

5. Conclusion

The instability of hydraulic jumps on sloping channels makes it challenging to regulate the jump. Utilizing bed appurtenances, altering the cross-section, and changing the layout of basins can help control and lower the building cost. Stilling basin design and dimensions are significant economic aspects. Through experimental inquiry, the impacts of the channel slope on the fundamental characteristics of the jump were evaluated in this study.

According to the study, the incoming Froude number, Reynolds number, and channel slope all influence the jump's primary factors. The hydraulic jump on a sloping channel is unstable at high inflow Froude numbers, according to experimental data, which makes managing the hydraulic jump challenging. The acquired results were compared to experimental findings and findings from earlier research. Additionally, experimental data-based empirical prediction equations were put out to calculate the depth ratio, jump length, and energy loss.

It was found from the experimental observation that the depth ratio (d_2/d_1) rises with Fr_1 and channel slope θ also. The jump length L_j/d_1 rises with Fr_1 but it decreases with channel slope θ and d_1/d_2 also. The energy loss E_L/E_1 also increases with Fr_1 as well as with channel slope θ. As compared to the classical jump d_2/d_1 rises by approximately 34.85%, and L_j/d_1 decreases by approximately 18.91% for 6^0 channel slope. It was found from the experimental observation that energy loss is approximately 15.38%, 35.07% and 63.62% for 2^0, 4^0, and 6^0 channel slopes respectively as compared to

classical hydraulic jump (0^0 bed slopes). From here we can conclude that energy loss increases with the increase of bed slope which is the requirement in the case of the hydraulic jump phenomenon to minimize the adverse effect of this phenomenon to prevent the environment and also to increase environmental sustainability.

All the developed empirical correlations were valid for Fr_1 ranging between 2 to 10 and Re_1 ranging from 5100 to 26000. When the bed slope rose, the reduction became more noticeable. Last but not least, it should be mentioned that slopped channels function better by releasing excess energy from entering the flow and may be more efficient in preventing erosion and failure of the hydraulic structure downstream such as spillway, water treatment plant, dams, discharge measuring devices and many more hydraulic structures.

Nomenclature

d_1	Sloped channel pre-jump depth
d_2	Sloped channel post jump depth
E_1	Pre-jump energy per unit weight
E_2	Post jump energy per unit weight
E_L	Loss of energy due to the formation of jump
f	Function of
g	Gravitational acceleration
H_j	Height of jump
Re_1	Incoming Reynolds number
L_j	Jump length
L_r	Roller length
M_1	Momentum per second before the jump
M_2	Momentum per second after the jump
P_1	Hydrostatic force before the jump
P_2	Hydrostatic force after the jump
q	Discharge through the channel
R^2	Determination coefficient
V	The average velocity of flow
V_1	Pre-jump flow velocity
V_2	Post jump flow velocity
W	Weight of water in the jump
Y_1	Pre-jump flow depth in a horizontal bed
Y_2	Post jump flow depth in a horizontal bed

Greek symbols

ρ	Fluid density
μ	Viscosity of fluid
ε	Surface roughness
η	Efficiency of jump
θ	Channel Slope

References

1) N. Rajaratnam, "The hydraulic jump as a well jet," *Journal of the Hydraulics Division*, **91**(5) 107–132 (1965)
2) S. Ikuta, Y. Masuda, K. Matsui, H. Shimada, T. Sasaoka, "Development and Application of Ground Improvement Machinery Chain Conveyor Cutter," *Evergreen Journal of Novel Carbon Resource Sciences*, **7** 18-25 (2013).
3) N. Pourabdollah, M. Heidarpour, J. A. Koupai, "An experimental and analytical study of hydraulic jump over a rough bed with an adverse slope and a positive step," *Iranian Journal of Science and Technology, Transactions of Civil Engineering*, **43**(3) 551-561 (2019)
4) Warjito, O. Putrawan, Budiarso, R. Irwansyah, S. BS Nasution, "The numerical study of the effect of blade depth and rotor-basin ratio on vortex hydro turbine performance," *Evergreen*, **9**(2) 556-562 (2022).
5) M. W. AlShaar, Z. Al-Omari, W. Emar, M. Alnsour, G. Abu-Rumman "Application of pv-thermal array for pumping irrigation water as an alternative to pv in ghor al-safi, jordan: a case study," *Evergreen*, **9**(4) 1140-1150 (2022).
6) N. Hassanpour, S. Sadeghfam, B. Crookston, et al., "Predicting hydraulic jump characteristics in a gradually expanding stilling basin with roughness elements by Sugeno Fuzzy Logic," *Journal of Hydroinformatics*, **24** (3) 659–676 (2022).
7) F. Jiang, C. Hu, "Application of lattice Boltzmann method for simulation of turbulent diffusion from a CO_2 lake in deep ocean," *Evergreen Journal of Novel Carbon Resource Sciences*, **5**10-28 (2012).
8) P. L. Singh, B. S. Sikarwar, "Parametric performance of condensation factors for extracting potable water from atmosphere," *Evergreen*, **8**(3) 586-592 (2021).
9) E. Maryami, R. Mohammadpour, M. K. Beirami, et al., "Prediction of hydraulic jump characteristics in a closed conduit using numerical and analytical methods," *Flow Measurement and Instrumentation*, **82** 102071 (2021).
10) Y. Gunawan, V. Nurliyanti, N. Akhiriyanto, et al., "A comparative study of photovoltaic water pumping systemdriving conventional ac single-phase and three-phase motor submersible pumps," *Evergreen*, **9**(3) 893-902 (2022).
11) A. Ghaderi, M. Dasineh, F. Aristodemo, et al., "Characteristics of free and submerged hydraulic jumps over different macroroughnesses," *Journal of Hydroinformatics*, **22** (6) 1554–1572 (2020).
12) M. Ardiclioglu, AMW Mohamed Hadi, E. Periku, et al., "Experimental and numerical investigation of bridge configuration effect on hydraulic regime," *International Journal of Civil Engineering*, **20** 981-991 (2022).
13) M. Dhar, S. Ray, G. Das, et al., "Hydraulic jump induced flooding and slugging in stratified gas-liquid flow – An experimental appraisal,"

Experimental Thermal and Fluid Science, **134** 110617 (2022).
14) D. Bonn, A. Andersen, T. Bohr, "Hydraulic jumps in a channel," *Journal of Fluid Mechanics*, **618** 71-87 (2009).
15) M. Kramer, D. Valero, "Turbulence and self-similarity in highly aerated shear flows: The stable hydraulic jump," *International Journal of Multiphase Flow*, **129** 103316 (2020).
16) A. N. AlTalib, A. Y. Mohammed, H. A. Hayawi, "Hydraulic jump and energy dissipation downstream stepped weir," *Flow Measurement and Instrumentation*, **69** 101616 (2019).
17) H. Askarizadeh, H. Ahmadikia, C. Ehrenpreis, et al., "Heat transfer in the hydraulic jump region of circular free-surface liquid jets," *International Journal of Heat and Mass Transfer*, **146** 118823 (2020).
18) E. Abushandi, "Experimental investigations of open-channel flow and velocity to develop a predictive tool from a laboratory small scale to real-world large scale," *Water Science & Technology*, **86** (7) 1681–1692 (2022).
19) K. Subramanya, "Flow in Open Channels," *Tata McGraw Hill Publishing Company Limited New Delhi* (1982)
20) W. H. Hager, "Energy dissipators and hydraulic jump," *Water Science and Technology Series Springer Dordrecht*, (1992).
21) J. N. Bradley, A. J. Peterka, "Hydraulic Design of Stilling Basins," *Journal of Hydraulic Division*, **83** 1404-1406 (1957).
22) V. T. Chow, "Open-Channel Hydraulics," *McGraw Hill New York* (1959).
23) S. Ead, N. Rajaratnam, "Hydraulic jumps on corrugated beds," *Journal of Hydraulic Engineering*, **128**(7) 656-663 (2002).
24) S. Pagliara, A. Peruginelli, "Limiting and sill-controlled adverse-slope hydraulic jump," *Journal of Hydraulic Engineering*, **126**(11) 847-851 (2000).
25) M. Beirami, M. R. Chamani, "Hydraulic jump in sloping channels: roller length and energy loss," *Canadian Journal of Civil Engineering*, **37**(4) 535–543 (2010).
26) S. Pagliara, M. Palermo, "Hydraulic jumps on rough and smooth beds: aggregate approach for horizontal and adverse-sloped beds," *Journal of Hydraulic Research*, **53**(2) 243–252 (2015).
27) M. Palermo, S. Pagliara,"D-jump in rough sloping channels at low Froude numbers," *Journal of Hydro-environment Research*, **14** 150-156 (2017).
28) A. Abbaspour, T. Taghavianpour, H. Arvanaghi, "Experimental study of the hydraulic jump on reverse bed with porous screens," *Applied Water Science*, **9**(7) 155 (2019).
29) G. Y. Luo, H. Cao, H. Pan, "Method to Locate the Toe of a Hydraulic Jump on Sloping Channels," *KSCE Journal of Civil Engineering*, **25** 124–139 (2021).
30) P. Parsamehr, A. Kuriqi, D. Farsadizadeh, et al., "Hydraulic jump over an adverse slope controlled by different roughness elements," *Water Resources Management*, **36** 5729–5749 (2022).
31) C-D Jan, C. J. Chang, "Hydraulic jump in inclined rectangular chute contraction," *Journal of Hydraulic Engineering*, **135**(11) 949-958 (2009).
32) J. A. McCorquodale, M. S. Mohamed, "Hydraulic jumps on adverse slopes," *Journal of Hydraulic Research*, **32**(1) 119–130 (1994).
33) K. Roushangar, F. Homayounfar, "Prediction characteristics of free and submerged hydraulic jumps on horizontal and sloping beds using SVM method," *KSCE Journal of Civil Engineering*, **23**(11) 4696–4709 (2019).
34) F. G. Carollo, V. Ferro, V. Pampalone, "Hydraulic jump on rough beds," *Journal of Hydraulic Engineering*, **133** 989–999 (2007).
35) W. H. Hager, R. Bremen, N. Kawagowshi, "Classical hydraulic jump: Length of roller," *Journal of Hydraulic Research*, **28** 591–608 (1990).
36) N. Hassanpour, A. H. Dalir, D. Farsadizadeh, et al., "An Experimental Study of Hydraulic Jump in a Gradually Expanding Rectangular Stilling Basin with Roughened Bed," *Water*, **9**(12) 945 (2017).
37) S. K. Gupta, R. C. Mehta, V. K. Dwivedi, "Modeling of Relative Length and Relative Energy Loss of Free Hydraulic Jump in Horizontal Prismatic Channel," **51** 529-537 (2013).
38) U. K. Singh, P. Roy, "Energy dissipation in hydraulic jumps using triple screen layers," *Applied Water Science*, **13** 17 (2023).

Appendix

Table 1 Summary of main parameters of experimental data of the present study

Experiments	θ (degree)	Q (m^3/s)	Fr_1	Re_1*10^5	d_1(m)	d_2(m)	V_1(m/s)	L_j (m)
1	0	0.00174-	2.51-	0.0828-	0.0119	0.0375-	1.099-2.196	0.246-0.526

		0.00475	7.57	0.2262		0.0755		
2	0	0.00186-0.00525	2.59-8.32	0.0937-0.2454	0.0162	0.0418-0.0796	1.253-2.324	0.251-0.532
3	2	0.00208-0.00525	2.57-7.61	0.09887-0.24989	0.0119	0.0545-0.0998	1.155-2.315	0.250-0.533
4	2	0.00226-0.00538	2.61-7.64	0.09925-0.25637	0.0162	0.0562-0.1203	1.257-2.323	0.253-0.541
5	4	0.00212-0.00532	2.56-7.62	0.10054-0.25277	0.0119	0.0646-0.1100	1.1478-2.3059	0.241-0.529
6	4	0.00238-0.00539	2.58-7.64	0.10578-0.25967	0.0162	0.0683-0.1251	1.1628-2.3425	0.249-0.543
7	6	0.00216-0.00550	2.73-7.58	0.10264-0.26138	0.0119	0.0745-0.1262	1.1232-2.2376	0.229-0.515
8	6	0.00232-0.00571	2.74-7.65	0.10572-0.28245	0.0162	0.0786-0.1302	1.1426-2.2564	0.0253-0.556